Water Science & Technology

IWA PUBLISHING

Water Science & Technology Vol 87 No 8, 2043 doi: 10.2166/wst.2023.110

Development of a mathematical model for a microbial denitrification co-culture system comprising acetogenic bacterium *Sporomusa ovata* and denitrifying bacterium *Pseudomonas stutzeri*

Haoyi Pei, Dan Chen*, Hongxia Jiang and Zhixing Xiao

College of Urban Construction, Nanjing Tech University, Nanjing 211816, China
*Corresponding author. E-mail: chendan1203@njtech.edu.cn

ABSTRACT

Previous study has shown that co-culturing acetogenic bacterium *Sporomusa ovata* (SO), with denitrifying bacterium *Pseudomonas stutzeri* (PS), is a promising strategy to enhance the microbial denitrification for nitrate-contaminated groundwater remediation. However, the mutual effects and reaction kinetics of these two bacteria in the co-culture system are poorly understood. In this study, a mathematical model for this co-culture system was established to fill this knowledge gap. Model simulation demonstrated that SO had a significant effect on the kinetics of denitrification by PS, while PS slightly affected the kinetics of acetate production by SO. The optimal initial HCO_3^-/NO_3^- ratio and SO/PS inoculation ratio were 0.77–1.48 and 67 for the co-culture system to achieve satisfied denitrification performance with less acetate accumulation. Finally, the minimum hydrogen supply was recommended when the initial bicarbonate and nitrate concentrations were assigned in the range of 2–20 mM and 2–4 mM for simulating the natural nitrate-contaminated groundwater treatment. These findings could provide useful insights to guide the operation and optimization of the denitrification co-culture system.

Key words: acetate accumulation, co-culture system, denitrification performance, mathematical model

HIGHLIGHTS

- A mathematical model for the co-culture system comprising *Sporomusa ovata* and *Pseudomonas stutzeri* was proposed.
- The mutual effects between these two bacteria were revealed.
- The optimal initial HCO_3^-/NO_3^- ratio was 0.77–1.48 for the co-culture system to achieve satisfied denitrification performance.
- The minimum hydrogen supply was simulated under different bicarbonate and nitrate concentration conditions.

NOMENCLATURE

n_{H_2}	Total amount of hydrogen
r	The net reaction rate of substrate, mol/(mol·s)
$r_{H_2,aq}$	Specific rate for dissolved hydrogen consumption
p	The partial pressure of hydrogen gas, Pa
$S_{H_2,aq}$	The concentration of hydrogen in the liquid phase, mol/m^3
ΔG	Gibbs energy, J
ΔG_e	Gibbs energy generated per mole of electrons, J/mol
γ	The reduction degree
ρ	Absolute reaction rate

Abbreviations

SO	*Sporomusa ovata*
PS	*Pseudomonas stutzeri*
CAT	Catabolic reaction
Max	Maximum
COD	Chemical oxygen demand

Superscripts

0 Standard reference conditions (1 mol/L, 1 atm, 298 K)
01 Biochemical reference conditions (pH 7)

1. INTRODUCTION

Nitrate contamination in groundwater has become a global problem (Gao *et al.* 2020), which is often caused by anthropogenic activities such as excess fertilizer application in agricultural fields and improper discharge of sewage or treated wastewater (Mencio *et al.* 2016; Yang & Toor 2017). Considering that high concentration of nitrate would pose threats to aquatic ecosystems and public health, such as eutrophication of water bodies and methemoglobinemia in infants (Capodici *et al.* 2018), the World Health Organization (WHO) has set a recommended maximum contaminant level (MCL) of 11 mg/L NO_3^--N in drinking water, and the United States Environmental Protection Agency (USEPA) promulgates a lower enforceable MCL of 10 mg/L NO_3^--N (Garcia-Segura *et al.* 2018).

To date, many methods have been developed to treat nitrate-contaminated groundwater (Lazaratou *et al.* 2020). Compared to physicochemical methods such as reverse osmosis (Epsztein *et al.* 2015; Talalaj 2015) and chemical reduction (Hosseini *et al.* 2018), biological denitrification has been widely applied due to its cost-effectiveness, high nitrate removal efficiency, and environmental-friendliness (Costa *et al.* 2018; Rezvani *et al.* 2019). Biological denitrification can be divided into autotrophic denitrification and heterotrophic denitrification depending on the electron donor/carbon source used. Heterotrophic denitrification using organic compounds (e.g., acetate) is considered as a more effective and operable approach in the field compared to autotrophic denitrification using inorganic compounds (e.g., sulfide) (Di Capua *et al.* 2019). However, the addition of excessive organic electron donors to groundwater may lead to excessive biomass growth and may further clog the aquifer. In addition, residual organics and metabolites may cause secondary contamination of groundwater (Amoako-Nimako *et al.* 2021).

In our previous study, a co-culture system consisting of an acetogenic bacterium *Sporomusa ovata* (DSMZ2662) and a denitrifying bacterium *Pseudomonas stutzeri* (JCM20778) achieved denitrification using H_2 as the sole external electron donor and CO_2 as the sole external carbon source, where *S. ovata* (SO) used H_2 and CO_2 to produce acetate for supporting microbial denitrification by *P. stutzeri* (PS) (Xiao *et al.* 2016). The advantage of this co-culture system is that it provides organic substrates through a slow-released microbial process rather than by direct addition, allowing more effective use of substrates. The good performance and stability of the denitrification activity of the co-culture system was demonstrated by a long-term test of 61 days. However, it has not been validly assessed whether the instability of acetate production was related to SO/PS inoculation ratio, and the influence of the important factors on further improving the denitrification performance and how to control the acetate concentration in the co-culture system is also unclear. Understanding these issues by experimental means is a tedious and time-consuming process, which also cannot provide a comprehensive study on the interactive behavior between SO and PS, as well as their reaction kinetics.

Mathematical modeling is a useful tool to predict the substrates changes and microbial community shifts, analyze the interactive effect of the dynamic factors, optimize the multi-species system performance, and provide strong support for understanding the impact of the key factors and their trade-offs in a complex system. Recently, Kubannek *et al.* (2020) established a mathematical simulation model to describe the substrate consumption and metabolite production in a co-culture system of *Raoultella electrica* and *Geobacter sulfurreducens* and further to gain quantitative insights into the biochemical process and to identify the limiting factors of the co-culture system. Chen *et al.* used a mathematical model to investigate the development of an integrated microbial community containing anammox bacteria, denitrifying anaerobic methane oxidation (DAMO) archaea, and DAMO bacteria under different operational conditions, and further to identify the key limiting factors, to optimize the system performance, and to reveal the cooperation between multi-species (Chen *et al.* 2016). Although current existing models have been demonstrated to describe the substrate consumption and predict the performance of the multi-species system, little effort has been dedicated to model the interactive behavior between the multi-species, which is very helpful for understanding the underlying mechanisms.

Therefore, based on our previous work (Xiao *et al.* 2016), we established a mathematical model of a microbial denitrification co-culture system consisting of SO and PS for the first time to investigate the biomass variation of SO and PS in the co-culture system and to comprehensively explore the denitrification performance of the co-culture system under different substrate concentrations and SO/PS inoculation ratio conditions. The novelty of our model differed from other studies was that

we emphasized the interactive metabolic behaviors of the two species and comprehensively analyzed the mutual effects between the two species. The main simulation objectives are (1) investigating the effect of SO on the denitrification reaction of PS by varying single parameter of the acetate production substrates of SO (SO biomass, hydrogen, bicarbonate), and the effect of PS on the acetate production reaction of SO by varying a single parameter of the denitrification reaction substrates of PS (PS biomass, nitrate) to reveal the mutual influences between SO and PS; (2) exploring the effects of bicarbonate to nitrate ratio and SO/PS inoculation ratio on the denitrification performance of the co-culture system; (3) evaluating the minimum hydrogen supply of the co-culture system for treating simulated natural nitrate-contaminated groundwater.

2. METHODOLOGY

2.1. Model description

2.1.1. Model assumption

This co-culture system consisted of two parts (Figure 1): the gas phase and the liquid phase. We assumed that all types of substances in the system were well mixed. The components in the gas phase were hydrogen, carbon dioxide, and nitrogen gas, which did not chemically react with each other. The soluble hydrogen, bicarbonate, acetate, nitrate, and biomass were the components in the liquid phase. SO could only convert bicarbonate to acetate by using hydrogen as an electron donor, and PS could only utilize the produced acetate as carbon source and electron donor for microbial denitrification in the co-culture system.

2.1.2. Microbial growth coefficient equation

The bacterial growth model was established based on the metabolic reactions of the two species (Equations (1) and (2), and the associated parameters were listed in Table 1, the microbial growth coefficient equation was equated according to Heijnen & Kleerebezem (2010).

SO:

$$18.18H_2 + 9.04HCO_3^- + 4.82H^+ + 0.2NH_4^+ \rightarrow 1CH_{1.8}O_{0.5}N_{0.2} + 4.02CH_3COO^- + 18.58H_2O \quad (1)$$

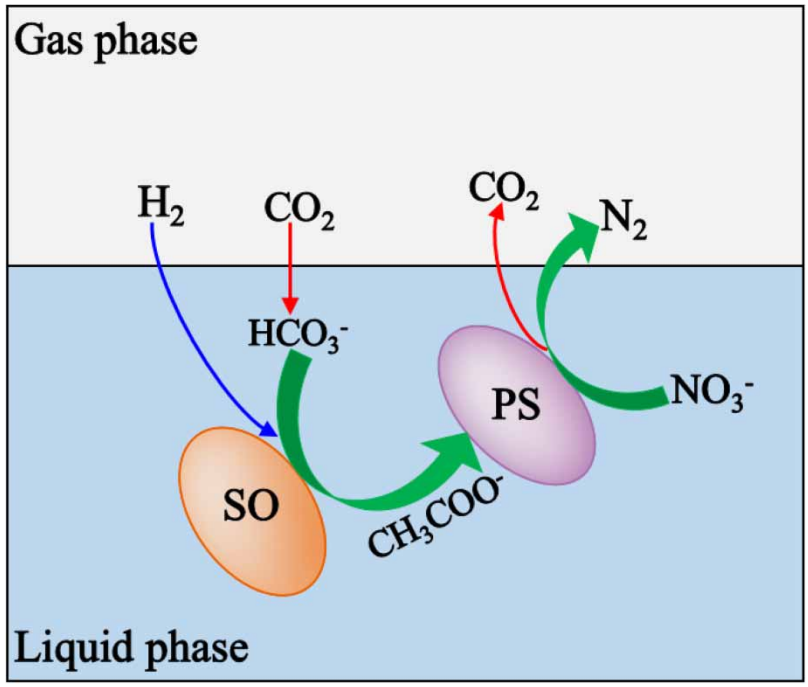

Figure 1 | Metabolic reactions of the two species in the co-culture system.

Table 1 | Parameters for the model

Parameter	Definition	Values	Unit
Calculation constants			
V_{aq}	The volume of liquid phase[a]	0.02	L
V_{gas}	The volume of gas phase[a]	0.04	L
R	Ideal gas constant	8.314	mM Pa K^{-1}
T	The temperature of this system	298.15	K
H^{cp}	Henry's constant for hydrogen[b]	7.8×10^{-6}	mM/Pa
β	The volume ratio of gas to liquid[a]	2	Dimensionless
Stoichiometric coefficients			
$Y_{HCO_3^-,1}$	Yield bicarbonate from SO-substrate[c]	0.4972	(mmol bicarbonate) (mmol hydrogen)$^{-1}$
Y_{X_1}	Yield SO biomass on substrate[c]	0.055	(mmol C SO – biomass) (mmol hydrogen)$^{-1}$
$Y_{Ac,1}$	Yield acetate from SO-substrate[c]	0.2211	(mmol acetate) (mmol hydrogen)$^{-1}$
$Y_{NO_3^-}$	Yield coefficient from PS-substrate[c]	0.8186	(mmol nitrate) (mmol acetate)$^{-1}$
Y_{X_2}	Yield PS biomass on substrate[c]	0.9302	(mmol C PS – biomass) (mmol acetate)$^{-1}$
$Y_{HCO_3^-,2}$	Yield bicarbonate from PS-substrate[c]	1.0698	(mmol bicarbonate) (mmol acetate)$^{-1}$
Y_{N_2}	Yield nitrogen from PS-substrate[c]	0.4093	(mmol nitrogen) (mmol acetate)$^{-1}$
System components (initial default value)			
n_{0,H_2}	The total initial default amount of hydrogen[d]	0.26	mmol
S_{0,HCO_3^-}	Initial default bicarbonate concentration[e]	4	mM
$X_{0,1}$	Initial SO concentration[f]	0.03	mol C/m^3
$X_{0,2}$	Initial PS concentration[f]	3×10^{-4}	mol C/m^3
S_{0,NO_3^-}	Initial default nitrate concentration[d]	1.5	mM

[a]From Xiao *et al.* (2016).
[b]From Sander (2015).
[c]Calculated from stoichiometric coefficient based on Equations (1) and (2).
[d]Calculated from Xiao *et al.* (2016).
[e]Based on Wu & Sun (2016).
[f]Calculated from Picioreanu *et al.* (2007).

PS:

$$1.075CH_3COO^- + 0.88NO_3^- + 0.605H^+ + 0.2NH_4^+ \rightarrow 1CH_{1.8}O_{0.5}N_{0.2} + 1.15HCO_3^- + 0.44N_2 + 0.84H_2O \quad (2)$$

2.1.3. Gas–liquid distribution of hydrogen

Due to that bicarbonate rather than carbon dioxide was the substrate for SO, and the produced nitrogen gas had no effect on the co-culture system, we only considered the gas–liquid distribution of hydrogen in the co-culture model.

The diffusion rate constant of hydrogen in water was k_d ($k_d = 2 \times 10^{-5}$ mmol s^{-1} cm^{-2}) (Aoki *et al.* 2012). We set the interfacial area of the gas–liquid substance exchange in the co-culture system, i.e., the serum bottle, to be A (Equation (3)).

$$A = \pi \times c^2 \tag{3}$$

where c is the radius of the serum bottle, $c = 2$ cm. Based on Equation (3), the hydrogen diffusion rate was 21.7 mmol/day in the co-culture system. The maximum hydrogen consumption rate by SO was 0.04 mmol/day (data from condition 5 (Figure 2(e) in Xiao *et al.* 2016)), which was lower than 21.7 mmol/day. Thus, we simplified that the amount of the total hydrogen in the co-culture system was always equal to its amount in the gas phase (normally applied to the systems with low biomass or low hydrogen consumption rates). Therefore, the total hydrogen consumption in the co-culture system was expressed as in the following equation.

$$\frac{dn_{H_2}}{dt} = r_{H_2,aq} \times V_{aq} \tag{4}$$

Equations (5) and (6) could be obtained from the ideal gas equation and Henry's law.

$$p = \frac{RT}{V_{gas}} \times n_{H_2} \tag{5}$$

$$S_{H_2,aq} = H^{cp} \times p \tag{6}$$

The gas–liquid distribution equation for hydrogen gas was as given in the following.

$$S_{H_2,aq} = H^{cp} \times \frac{RT}{V_{gas}} \times n_{H_2} \tag{7}$$

2.1.4. Mass balances in bulk liquid

Regarding the soluble components (e.g., nitrate, bicarbonate) in the system, we assumed that S_B was the concentration of any soluble component, and the ordinary differential equation represented the mass balance in the bulk liquid was:

$$\frac{dS_B}{dt} = r_B \tag{8}$$

The specified initial conditions $S_B(t = 0) = S_0$ for all soluble components. r was the net reaction rate of substrate utilization by microorganisms (SO and PS).

2.1.5. Microbial reaction kinetics

The microbial reaction kinetics was based on the Monod dual-substrate model, and the model was represented in the form of a stoichiometric matrix, as shown in Table 2. The rows listed the kinetic processes, while the columns listed the components involved in these processes.

The ordinary differential equation of hydrogen consumption in the gas phase (Equation (9)) could be obtained according to Table 2.

$$\frac{dn_{H_2}}{dt} = -V_{aq} \times q_{H_2,max} \times \frac{H^{cp} \times \frac{RT}{V_{gas}} \times n_{H_2}}{\left(K_{H_2} + H^{cp} \times \frac{RT}{V_{gas}} \times n_{H_2}\right)(1 + H\beta)} \times \frac{S_{HCO_3^-}}{K_{HCO_3^-} + S_{HCO_3^-}} \cdot X_1 \tag{9}$$

The fundamental model was implemented with MATLAB 2018. In the MATLAB base script file, we defined the biological, physical, and chemical parameters relevant to this model and established the preliminary model framework. The model parameters were adjusted, and some of the scripts were modified depending on the research objectives.

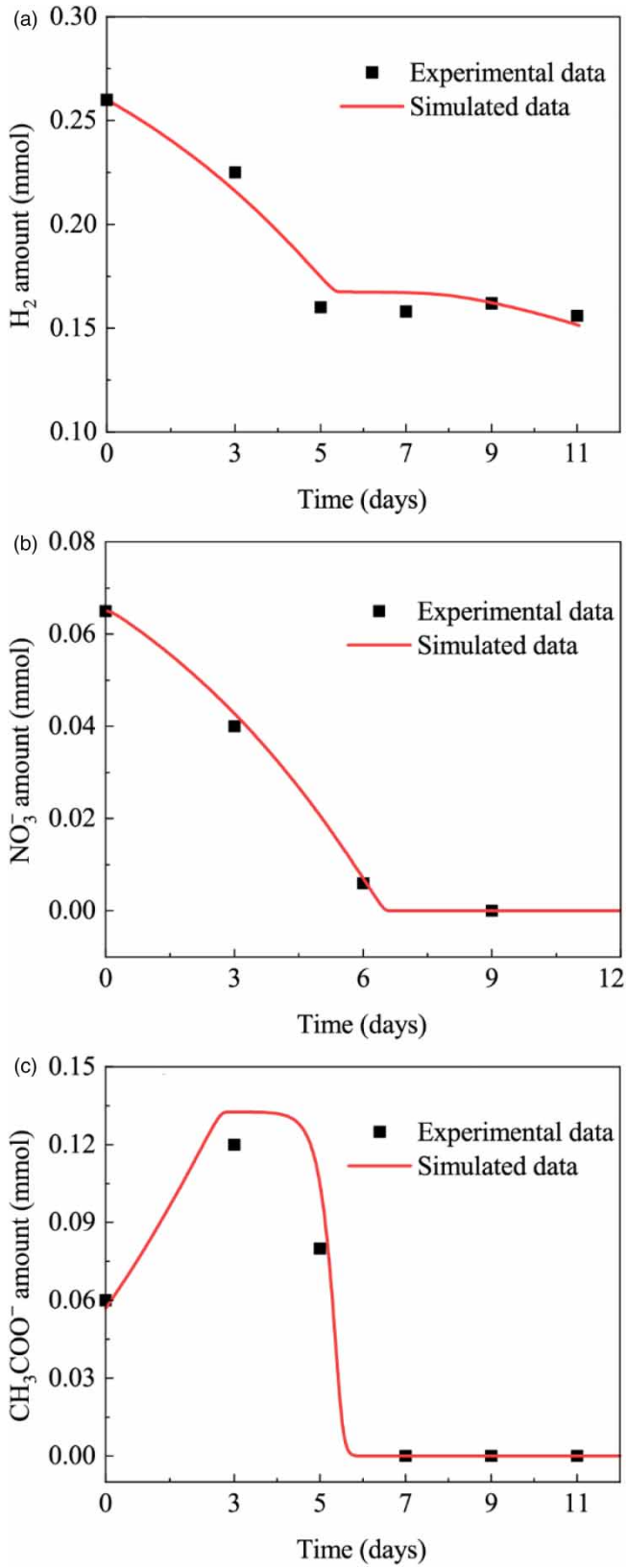

Figure 2 | Model calibration with experimental data of hydrogen (a) and nitrate (b) consumptions, and acetate accumulations (c) in the co-culture system (hydrogen consumption and acetate accumulation data from condition 2 (Figure 2B in Xiao *et al.* 2016), nitrate consumption data from long-term test (Figure 4 (day 0–12) in Xiao *et al.* 2016)).

Table 2 | Stoichiometric matrix of the co-culture system

Component → j	I Process ↓	1 n_{H_2}	2 $S_{HCO_3^-}$	3 S_{Ac^-}	4 $S_{NO_3^-}$	5 X_1	6 X_2	Reaction rate (ρ_j)
1	Autotrophic growth of SO	-1	$-Y_{HCO_3^-,1}$	$Y_{Ac,1}$		Y_{X_1}		$\rho_1 = -V_{aq} \times q_{H_2,max} \times \frac{H^{cp} \times \frac{RT}{V_{gas}} \times n_{H_2}}{(K_{H_2} + H^{cp} \times \frac{RT}{V_{gas}} \times n_{H_2})(1+H\beta)} \times \frac{S_{HCO_3^-}}{K_{HCO_3^-} + S_{HCO_3^-}} \cdot X_1$
2	Heterotrophic growth of PS		$Y_{HCO_3^-,2}$	-1	$-Y_{NO_3^-}$		Y_{X_2}	$\rho_2 = q_{Ac,max} \times \frac{S_{Ac}}{K_{Ac} + S_{Ac}} \times \frac{S_{NO_3^-}}{K_{NO_3^-} + S_{NO_3^-}} \cdot X_2$

2.2. Model calibration

The experimental data of hydrogen consumption and acetate accumulation from condition 2 (Figure 2(b) in Xiao *et al.* 2016), nitrate consumption from long-term test (Figure 4 (day 0–12) in Xiao *et al.* 2016), were used for model calibration. The default initial SO and PS biomass amounts and the substrate concentrations were adjusted to be consistent with the experimental conditions (Xiao *et al.* 2016). The predicted hydrogen, acetate, and nitrate concentrations based on the model and the measured experimental data were illustrated in Figure 2. The agreement between the predicted and measured data indicated that the constructed model could properly describe the substrates consumptions and microbial reactions in co-culture system. In addition, the parameter values for the optimum model fittings with the measured experimental data were listed in Table 3. Similar to the study of Kubannek & Krewer (2019), the parameter identification procedure was carried out through the log-likelihood function to minimize the deviation between the model output and the experimental data.

2.3. Model simulation

The kinetic equations of the two species were coupled for simulation. We investigated the mutual effects of the two species, specifically the effects of SO biomass amount, initial hydrogen supply, and initial bicarbonate concentration on the kinetics of the denitrification reaction by PS, and the effects of PS biomass amount, initial nitrate concentration, PS inoculation time on the kinetics of the acetate-producing reaction by SO. After that, the ratio of nitrate removal amount to hydrogen consumed amount ($\triangle NO_3^-/\triangle H_2$, which represents the denitrification co-culture system performance, larger value means better performance) was simulated under different substrate concentrations and inoculation conditions for predicting the co-culture system performance. Finally, the initial bicarbonate and nitrate concentrations were set in the range of 2–20 mM and 2–4 mM (natural nitrate-contaminated groundwater condition), and the minimum hydrogen supply was simulated.

The initial bicarbonate and nitrate concentrations for simulation at different scenarios were selected according to the reported values of the natural nitrate-contaminated groundwater (Tsai *et al.* 2004; Wick *et al.* 2012; Wang & Chu 2016; Wu & Sun 2016). The initial hydrogen amounts for simulation were selected after preliminary simulation, and the selected values could indicate significant changes in the co-culture system performance. The initial biomass amounts of PS and SO were selected by referring to the experimental data from our previous study (Xiao *et al.* 2016) and relevant literatures (Picioreanu *et al.* 2007). After the reaction, the ultimate nitrate concentration would not exceed 0.7 mM (9.8 mg/L NO_3^--N, meeting the drinking water standard of WHO) and the accumulated acetate concentration would not exceed 0.5 mM (10 mg/L COD).

Table 3 | Kinetic parameters for the model calibration

Parameter	Definition	Typical values	Calibrated values	Unit
$q_{H_2,max}$	Maximum specific rate constant for hydrogen consumption	2.8[a]	2.952	(mmol hydrogen) (mmol C biomass)$^{-1}$ day^{-1}
K_{H_2}	Monod half-saturation coefficient for substrate hydrogen	2.3×10^{-3}[a]	2.3×10^{-3}	mM
$K_{HCO_3^-}$	Monod half-saturation coefficient for substrate bicarbonate	0.02[b]	0.02	mM
$q_{Ac,max}$	Maximum specific rate constant for acetate consumption	5.2[c]	5.25	(mmol acetate) (mmol C biomass)$^{-1}$ day^{-1}
K_{Ac}	Monod half-saturation coefficient for substrate acetate	1.8[d]	1.954	mM
$K_{NO_3^-}$	Monod half-saturation coefficient for substrate nitrate	0.04[d]	0.044	mM

[a]Calculated from London *et al.* (2011).
[b]From Kazemi *et al.* (2015).
[c]Calculated from Picioreanu *et al.* (2007).
[d]Calculated from Feng *et al.* (2020).

3. RESULTS AND DISCUSSION

3.1. Effect of SO on the denitrification reaction by PS

3.1.1. Effect of initial SO biomass amount on the denitrification reaction by PS

Figure 3 shows the changes in nitrate concentration and PS biomass amount over time as the initial SO biomass amount varied (Figure 3(a) and 3(b)). The lag phase of the denitrification reaction by PS was shortened along with the increased initial SO biomass amount (Figure 3(a)). For instance, when the initial SO biomass amount increased from 0.03 to 0.3 mol C/m^3, the lag phase of the denitrification reaction by PS was decreased from 11 to 6.8 days. The significant effect of the initial SO biomass amount on the denitrification reaction by PS may be due to that the higher initial SO biomass amount accelerated the acetate supply for supporting microbial denitrification by PS (Figure S1 in Supplementary material). Notably, the accumulated acetate concentrations were closed to zero and remained stable from days 15 to 18 and days 13 to 15 when the initial SO biomass amounts were 0.03 and 0.06 mol C/m^3, respectively (Figure S2a in Supplementary material). This might be attributed to that the rate of acetate production by SO was equal to the rate of acetate consumption by PS during that period.

3.1.2. Effect of hydrogen supply and bicarbonate concentration on the denitrification reaction by PS

Figure 4(a) and 4(b) illustrates the effect of hydrogen supply on the nitrate removal and biomass growth of PS. Generally, both nitrate removal and PS biomass growth were accelerated when the initial hydrogen amount increased from 0.052 to 0.26 mmol, which may be due to the enhanced acetate production (Figure S3 in Supplementary material). Because other substrates were sufficient (Figure 4(a) and Figure S4 in Supplementary material), hydrogen amount might be the only limiting factor for PS denitrification reaction when its value was lower than 0.26 mmol. However, when the initial hydrogen amount was higher than 0.26 mmol, the denitrification reaction by PS did not continue to be accelerated. This indicates that hydrogen did not limit the PS denitrification reaction when its value exceeded 0.26 mmol. Under such conditions, bicarbonate concentration might limit the PS denitrification reaction. In addition, the half-saturation constant of hydrogen was estimated as 0.058 mmol, and the reaction kinetics would become zero order when the initial hydrogen amount was higher than 0.21 mmol, which explains why the rates of reaction at initial hydrogen amounts of 0.26 and 0.52 mmol were the same.

The effect of the initial bicarbonate concentration on the kinetics of the denitrification reaction by PS was similar to that of hydrogen supply (Figure 4(c) and 4(d)). When the initial bicarbonate concentration increased from 0.8 to 4 mM, the PS

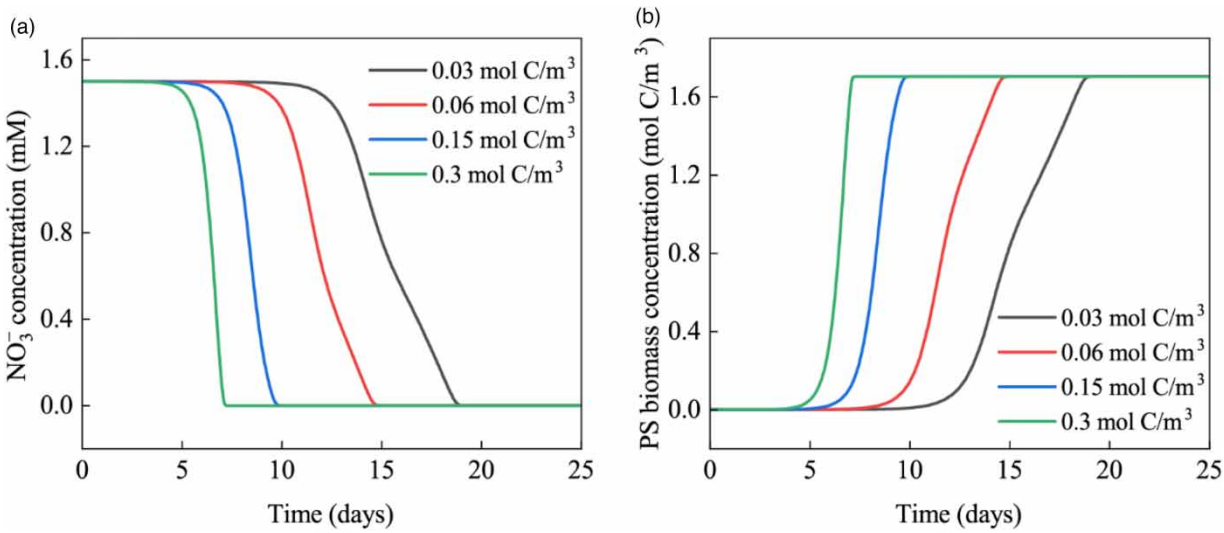

Figure 3 | Nitrate removal (a) and PS biomass growth (b) under different initial SO biomass amount conditions (the initial hydrogen amount was 0.26 mmol, the initial bicarbonate concentration and nitrate concentration were 4 and 1.5 mM, and the initial PS biomass amount was 3×10^{-4} mol C/m^3).

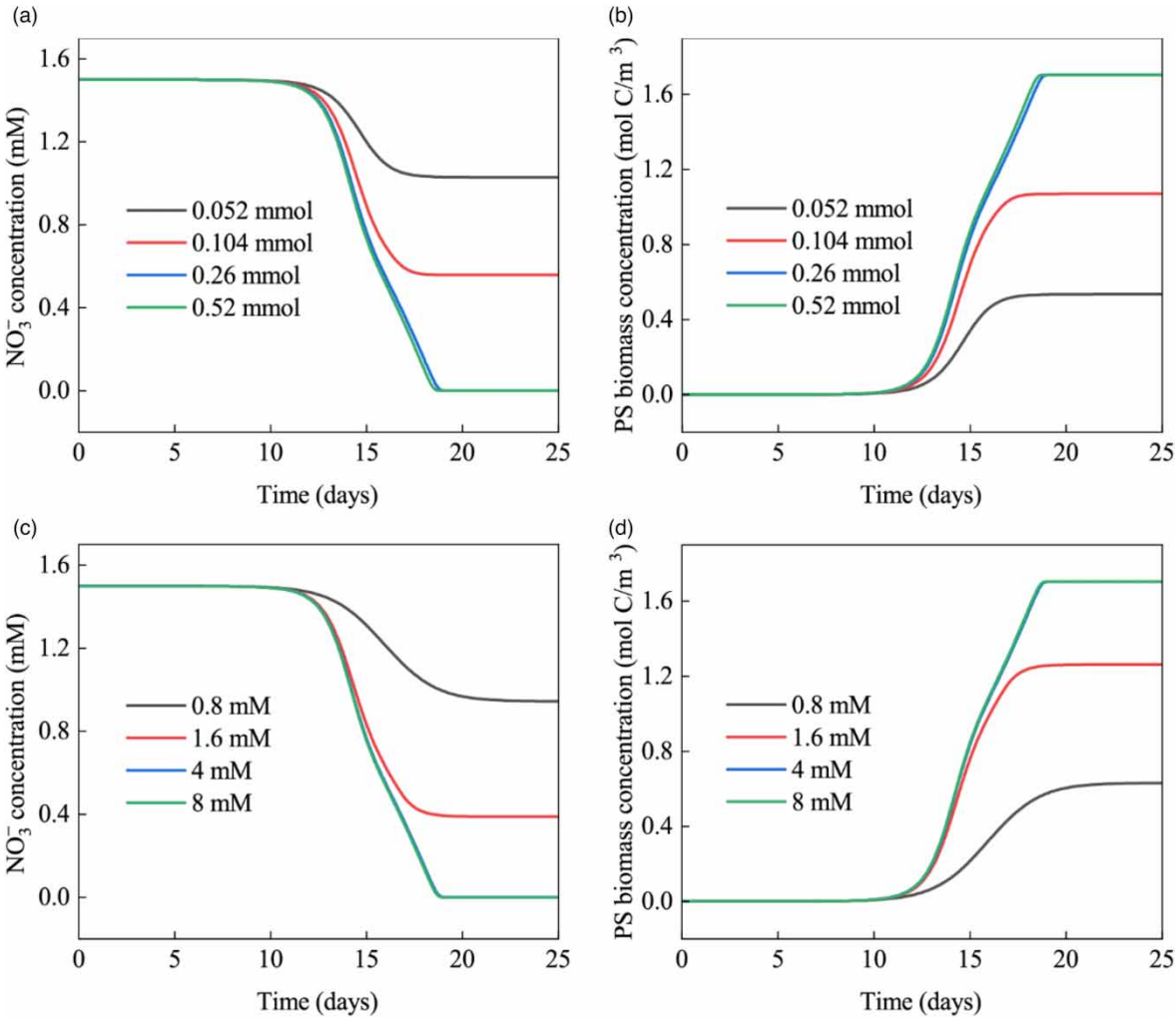

Figure 4 | Nitrate removal and PS biomass growth under different hydrogen supply (a,b) and initial bicarbonate concentration conditions (c,d) (the initial nitrate concentration was 1.5 mM, the initial SO and PS biomass amounts were 0.03 and 3×10^{-4} mol C/m^3 (a–d), the initial bicarbonate concentration was 4 mM (a,b), and the initial hydrogen amount was 0.26 mmol (c,d)).

biomass growth and nitrate removal were both accelerated, which was caused by the increased acetate production by SO (Figure S5 in Supplementary material). Because other substrates were sufficient (Figure 4(c) and Figure S6 in Supplementary material), bicarbonate concentration might be the only limiting factor for PS denitrification reaction when its value was lower than 4 mM. However, when the initial bicarbonate concentration increased to 8 mM, the PS biomass growth and nitrate removal did not continue to be accelerated and remained the same values with that of the initial bicarbonate concentration of 4 mM. This indicates that bicarbonate did not limit the PS denitrification reaction when its value exceeded 4 mM. Under such conditions, the hydrogen amount might limit the PS denitrification reaction. In addition, the half-saturation constant of bicarbonate was estimated as 1.06 mM, and the reaction kinetics would become zero order when the initial bicarbonate concentration was higher than 1.80 mmol.

Furthermore, we calculated the ratios of consumed hydrogen vs. produced nitrogen gas from the simulated data in Figure 4(a) (initial hydrogen amount was 0.26 mmol). When the acetate production rate by SO was equal to the acetate consumption rate by PS in the co-culture system, the calculated ratio of consumed hydrogen vs. produced nitrogen gas was 11.06, which was in accordance with the reaction stoichiometric ratio of 11.05. Such a finding also indicates that the simulated model results could properly reflect the expected reaction stoichiometry in the co-culture system.

3.2. Effect of PS on the acetate-producing reaction by SO

3.2.1. Effect of initial PS biomass amount on the acetate-producing reaction by SO

Figure 5 shows the effect of different initial PS biomass amount on the hydrogen and bicarbonate consumption, acetate accumulation, and SO biomass growth in the acetate-producing reaction by SO. Overall, the initial PS biomass amount had a slight effect on the reaction kinetics of SO. Hydrogen consumption and SO biomass growth showed no change with varied initial PS biomass amounts (Figure 5(a) and 5(c)). The bicarbonate concentration from day 10 to 15 presented an inflection point and the inflection point appeared earlier when the initial PS biomass amount was higher (Figure 5(b)), which was attributed to that the rate of bicarbonate produced by PS denitrification reaction was greater than the rate of bicarbonate consumption by SO during that period. Meanwhile, the maximum accumulated acetate appeared from day 8 to 16 and the maximum value decreased along with the increased initial PS biomass amount (Figure 5(d)). For instance, when the initial PS biomass amount increased from 3×10^{-4} to 3×10^{-3} mol C/m^3, the maximum accumulated acetate decreased from 0.57 to 0.35 mM. This may be due to that the higher initial PS biomass amount caused more rapid consumption of acetate for denitrification.

3.2.2. Effect of initial nitrate concentration on the acetate-producing reaction by SO

The effect of initial nitrate concentration on the acetate-producing reaction by SO is shown in Figure 6. As the initial nitrate concentration increased from 0.3 to 3 mM, the hydrogen consumption by SO and SO biomass growth both showed no change

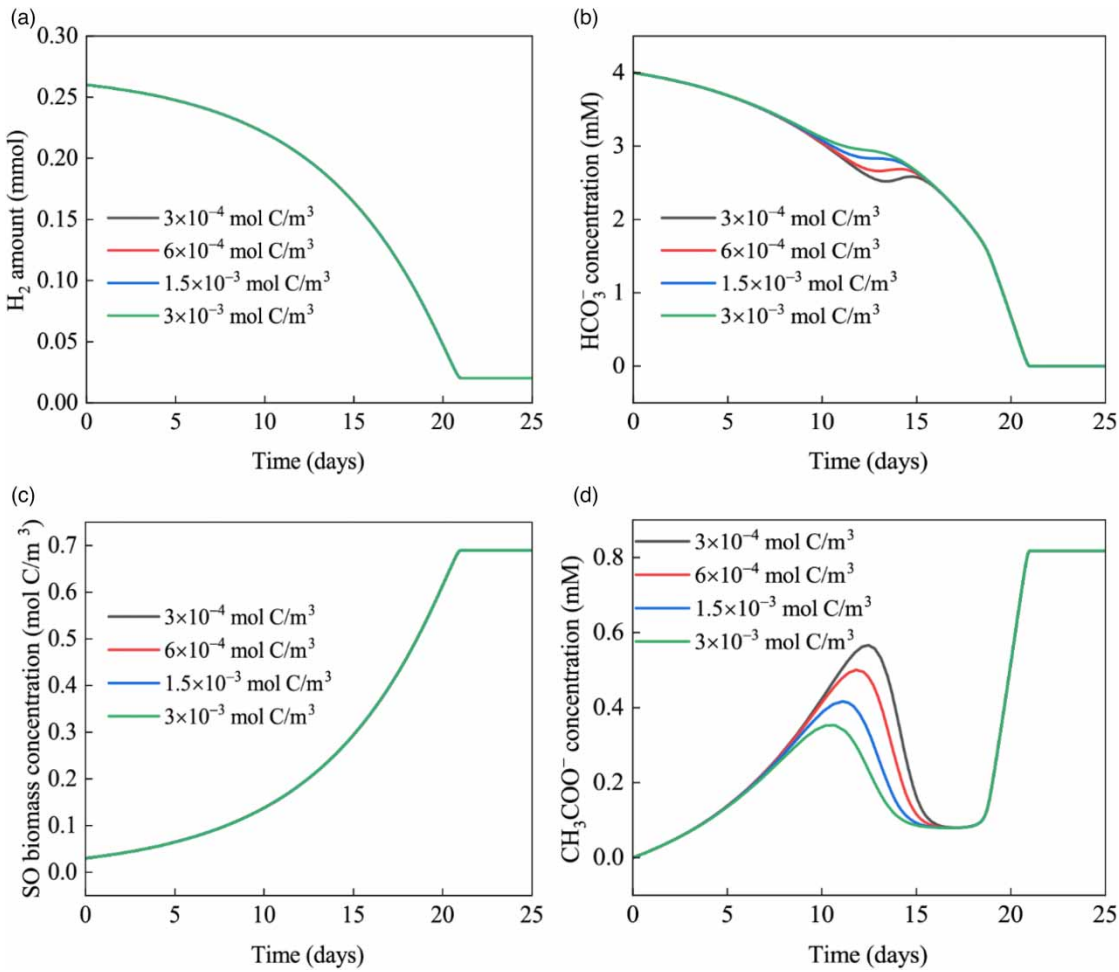

Figure 5 | Changes of hydrogen (a), bicarbonate (b), SO biomass (c), and acetate (d) concentrations over time under different initial PS biomass amount conditions (the initial hydrogen amount was 0.26 mmol, the initial bicarbonate concentration and nitrate concentration were 4 and 1.5 mM, and the initial SO biomass amount was 0.03 mol C/m^3).

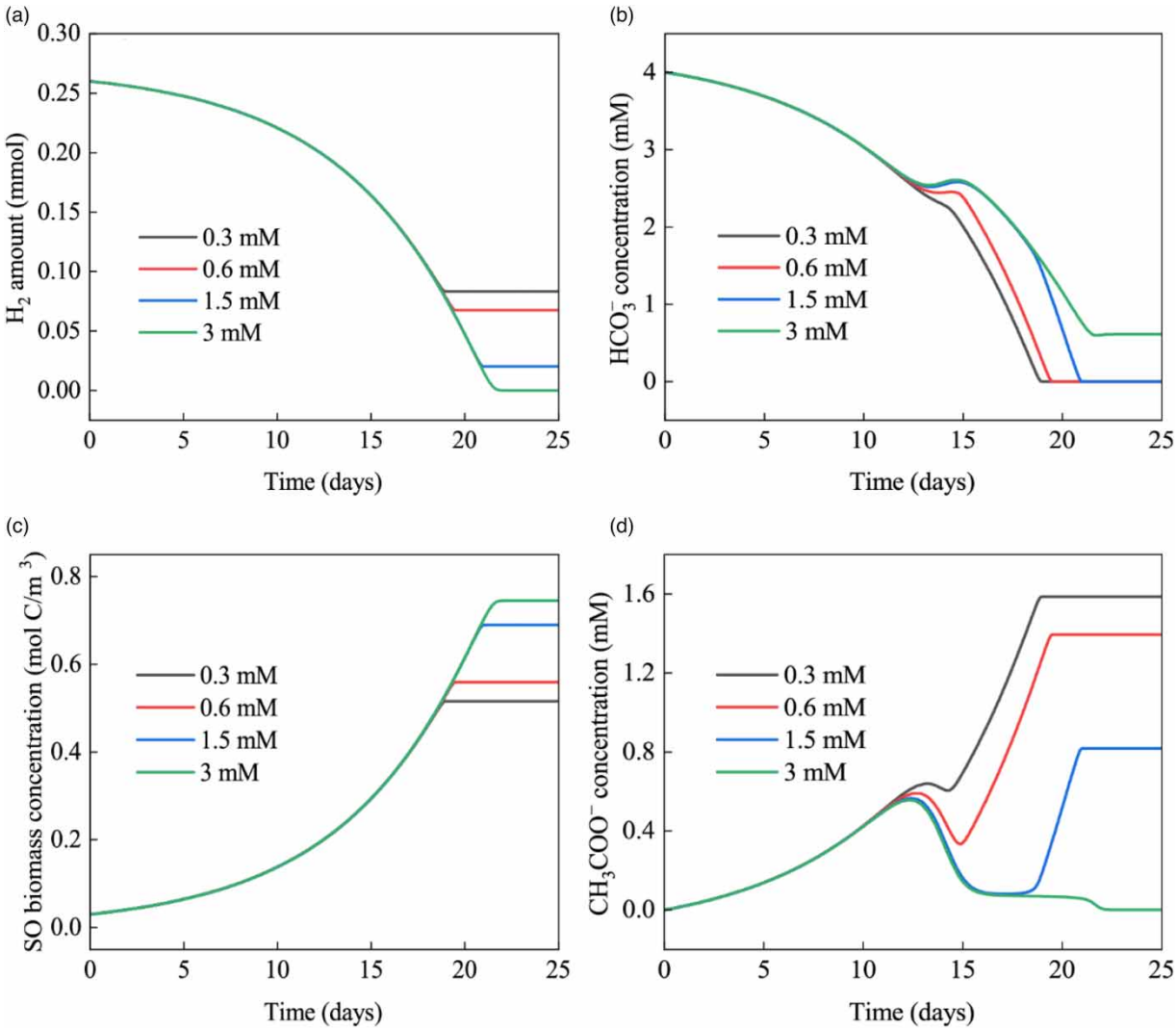

Figure 6 | Changes of hydrogen (a), bicarbonate (b), SO biomass (c), and acetate (d) concentrations over time under different initial nitrate concentration conditions (the initial hydrogen amount was 0.26 mmol, the initial bicarbonate concentration was 4 mM, and the initial SO and PS biomass amounts were 0.03 and 3×10^{-4} mol C/m^3).

except that the equilibrium time was prolonged (Figure 6(a) and 6(c)). However, the bicarbonate and acetate variations were both influenced by the varied initial nitrate concentration after 12 days (Figure 6(b) and 6(d)). There was a rising point in the bicarbonate concentration and a drop point in the acetate concentration from day 12 to 15, and the increased degree and decreased degree both elevated along with the increased initial nitrate concentration. This may be due to that the increase of the initial nitrate concentration that promoted the denitrification reaction by PS, thereby accelerating the acetate consumption and producing much more bicarbonate.

3.2.3. Effect of different inoculation times of PS on the acetate-producing reaction by SO

As shown in Figure 7(c), the growth trend of SO biomass was divided into three phases: (1) 0–10 days, the retardation period; (2) 10–20 days, the rapid proliferation period; and (3) 20–35 days, the stable period. If PS was inoculated during the retardation period of SO (day 5 or day 10), there was no difference in the hydrogen consumption and SO biomass growth (Figure 7(a) and 7(c)). This was due to the relatively low growth rates of both SO and PS under insufficient substrate conditions. If PS was inoculated during the rapid proliferation period of SO (day 15 or 20), the accumulated acetate would greatly decrease because of the proliferation of PS. When inoculating PS on day 25, the acetate consumption pattern was

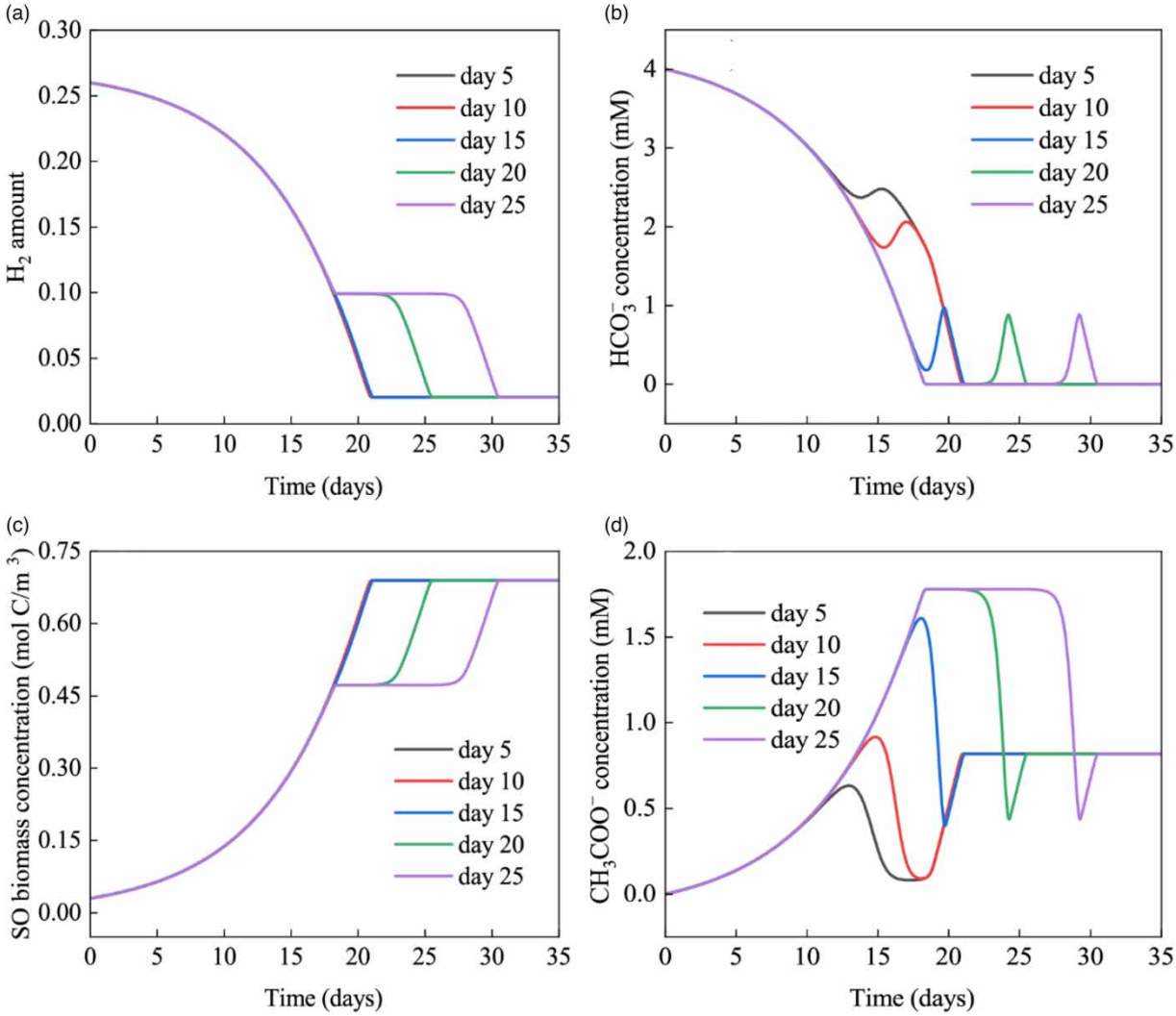

Figure 7 | Changes of hydrogen (a), bicarbonate (b), SO biomass (c), acetate (d) concentrations over time under different PS inoculation times (the initial hydrogen amount was 0.26 mmol, the initial bicarbonate concentration was 4 mM, the initial nitrate concentration was 1.5 mM, and the initial SO and PS biomass amounts were 0.03 and 3×10^{-4} mol C/m^3).

similar with that on day 20. Moreover, with the delay of the PS inoculation time, the accumulated acetate concentration was raised in the early stage, while the bicarbonate consumption accelerated (Figure 7(b) and 7(d)). Overall, the simulation strategies and results of Sections 3.1 and 3.2 were summarized in Table S1 in Supplementary material.

3.3. Predicting the co-culture system performance

3.3.1. System performance under different initial HCO_3^-/NO_3^- ratios

Figure 8(a) and 8(b) shows the variations of the $\triangle NO_3^-/\triangle H_2$ values and acetate accumulated concentrations in the co-culture system over time under different initial HCO_3^-/NO_3^- ratio (NO_3^- concentration was fixed) conditions. When the initial HCO_3^-/NO_3^- ratio increased from 0.5 to 1, the reaction time for the co-culture system to achieve the maximum $\triangle NO_3^-/\triangle H_2$ value was shortened from 23 to 18 days. Acetate would not accumulate after 21 days of reaction under these two HCO_3^-/NO_3^- ratio conditions. Therefore, increasing the HCO_3^-/NO_3^- ratio when its value was less than 1 could increase the denitrification rate of the system and reduce the accumulation of acetate in the early stage (Figure 8(b)). When the initial HCO_3^-/NO_3^- ratio further increased to 2.5 and 5, the variation of $\triangle NO_3^-/\triangle H_2$ values from day 0 to 18 was consistent with that at initial HCO_3^-/NO_3^- ratio of 1. However, the $\triangle NO_3^-/\triangle H_2$ values were then decreased and acetate

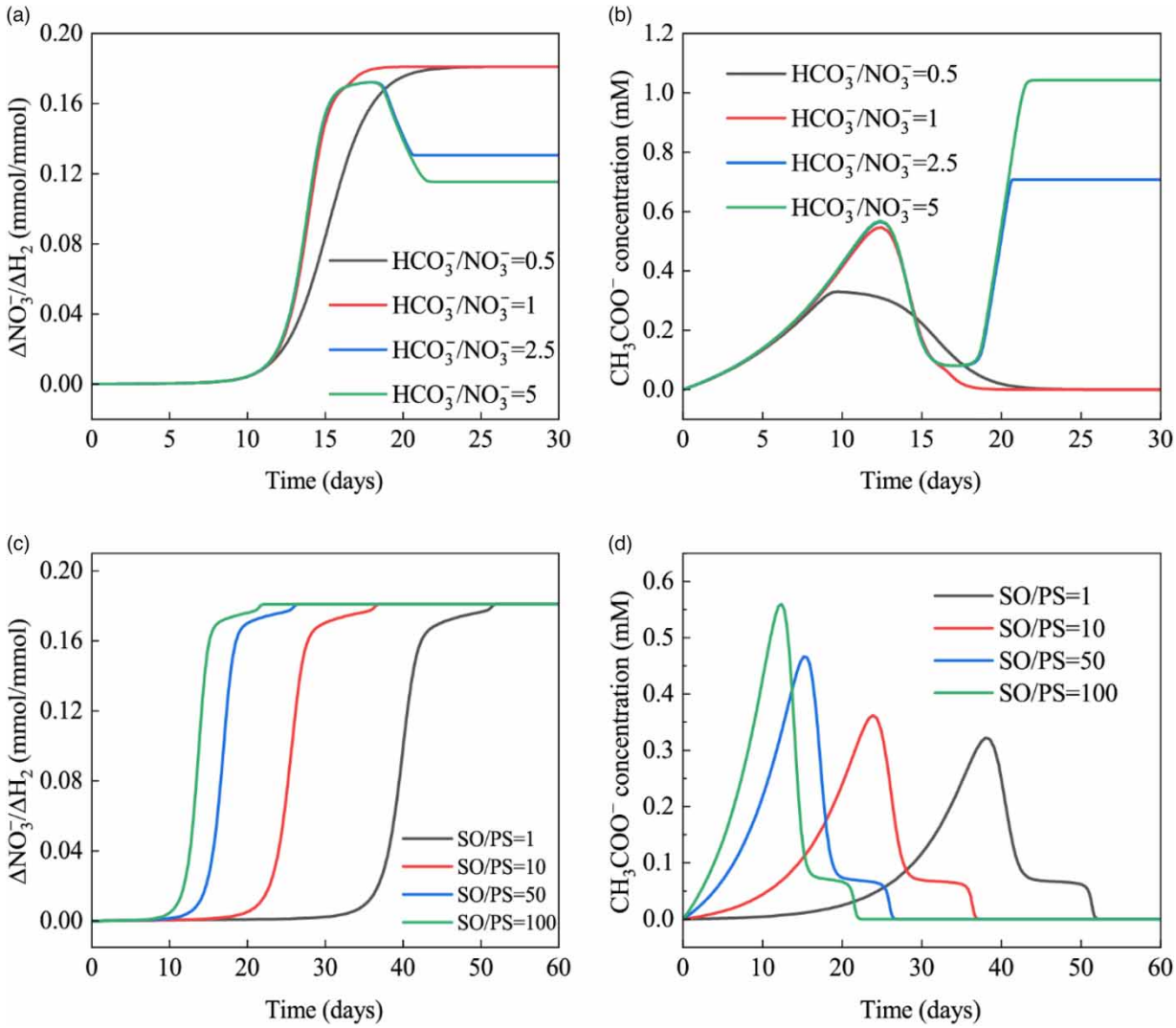

Figure 8 | $\triangle NO_3^-/\triangle H_2$ value changes over time in the co-culture system under different initial HCO_3^-/NO_3^- ratios (mmol/mmol) (a,b) (the initial hydrogen amount was 0.26 mmol, and the initial SO and PS biomass amounts were 0.03 and 3×10^{-4} mol C/m^3), and different SO/PS inoculation ratios (c,d) (the initial hydrogen amount was 0.26 mmol, the initial bicarbonate concentration was 4 mM, the initial nitrate concentration was 1.5 mM).

was rapidly accumulated after 18 days, which might be due to the depletion of nitrate in the co-culture system so that the remained bicarbonate could be used to produce acetate during that period under these two HCO_3^-/NO_3^- ratio conditions. Also, too high HCO_3^-/NO_3^- ratio can make acetate accumulation in the system uncontrolled. In the natural groundwater environments, excessive acetate accumulation may lead to secondary pollution and the reproduction of other heterotrophic microorganisms influencing the denitrification performance of the co-culture system. Therefore, the HCO_3^-/NO_3^- ratio was essential for the co-culture system. When we set the constraint condition that the reaction time for the co-culture system to achieve the maximum $\triangle NO_3^-/\triangle H_2$ value (denitrification performance) was achieved less than 25 days, the accumulated acetate concentration would not exceed 0.5 mM, and the ultimate nitrate concentration would not exceed 0.7 mM, the simulated optimal initial HCO_3^-/NO_3^- ratio for the co-culture system was in the range of 0.77–1.48. Similarly, Mousavi *et al.* investigated the effect of C/N (HCO_3^-/NO_3^-) ratio on the treatment of nitrate-polluted wastewater using autohydrogenotrophic denitrifying bacteria in a sequencing batch reactor, and they found that the reactor took a longer time to achieve complete denitrification at low C/N ratios of 1 or 2, while the nitrate reduction rate was decreased if the C/N ratio was increased from 4 to 8 (Mousavi *et al.* 2014).

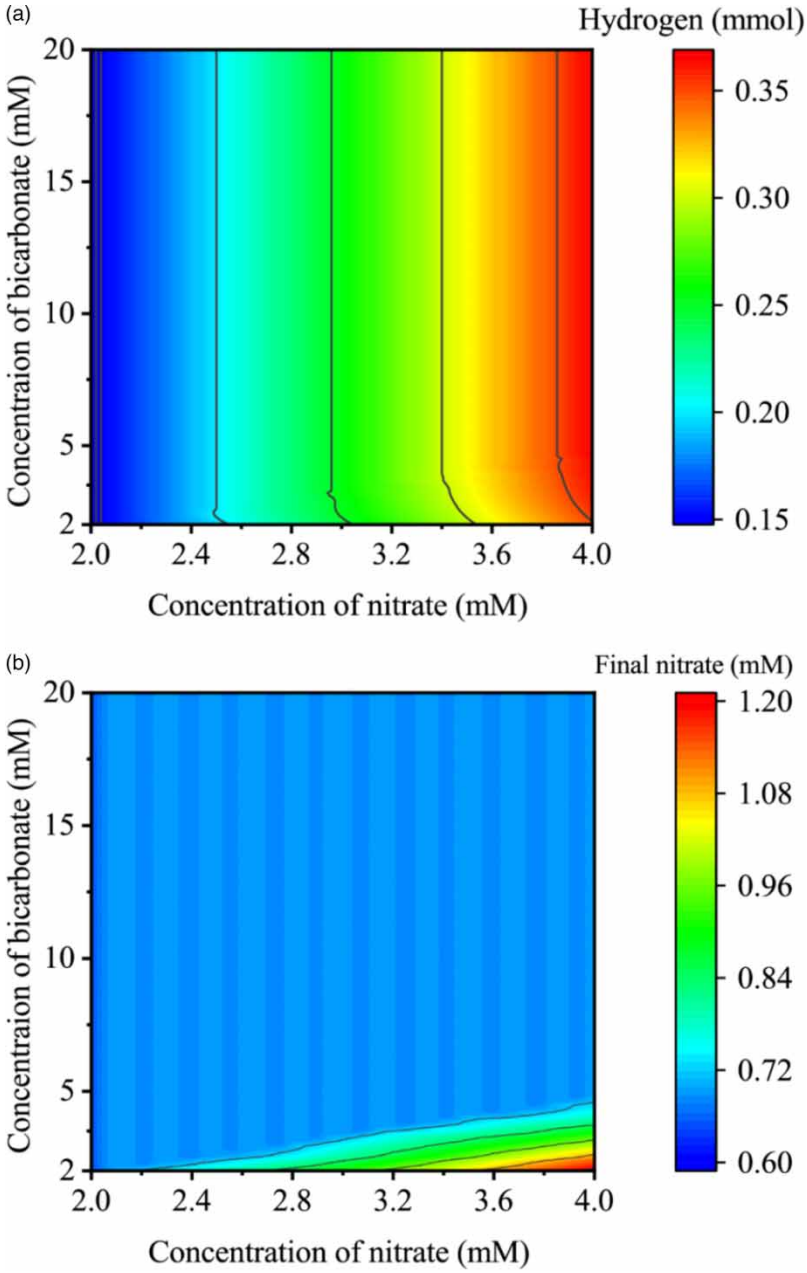

Figure 9 | Simulated minimum hydrogen supply (a) and corresponding terminal nitrate concentration after treatment (b) under different bicarbonate and nitrate concentrations in the co-culture system (the initial SO and PS biomass amounts were 0.03 mol C/m^3 and 3×10^{-4} mol C/m^3).

3.3.2. System performance under different SO/PS inoculation ratio conditions

Figure 8(c) and 8(d) shows the variations of $\triangle NO_3^-/\triangle H_2$ values and accumulated acetate concentrations in the co-culture system over time under different SO/PS inoculation ratio conditions. As the SO/PS inoculation ratio increased, the reaction time for the co-culture system to reach the maximum $\triangle NO_3^-/\triangle H_2$ value was shortened, and the acetate accumulated amount was increased. For instance, when the SO/PS inoculation ratio increased from 1 to 10, the reaction time for the co-culture system to reach the maximum $\triangle NO_3^-/\triangle H_2$ value was decreased from 52 to 36 days, while the maximum acetate accumulated concentration increased from 0.32 to 0.36 mM. Therefore, it is particularly important to control the SO/PS inoculation ratio in the co-culture system. Based on the simulation results, when we set the constraint condition that the

accumulated acetate concentration would not exceed 0.5 mM, the simulated optimal SO/PS inoculation ratio was 67 with the highest $\triangle NO_3^-/\triangle H_2$ value (denitrification performance) in the co-culture system. In our previous experimental study (Xiao *et al.* 2016), the acetate concentration was very low in the early stage of the long-term test, which was likely related to the lower initial SO/PS inoculation ratio because other substrates had slight effects on the acetate concentration from the simulation results in the present study (Figure 6(d), Figure 8(b) and Figure S4b). It seems that the intermediate product acetate could act as an indicator to regulate the SO/PS inoculation ratio in the co-culture system, which was similar to the indicator of VFA for regulating the methane production performance in anaerobic methanogenic systems (Lim *et al.* 2020).

3.4. Minimizing hydrogen supply under different bicarbonate and nitrate concentration conditions

For further application of this co-culture system for remediation of nitrate-contaminated groundwater, it is important to select the hydrogen supply amount under different bicarbonate and nitrate concentrations because too much hydrogen was costly (Tarhan & Cil 2021). We selected the initial bicarbonate concentration ranging from 2 to 20 mM and nitrate concentration ranging from 2 to 4 mM for simulating the natural nitrate-contaminated groundwater environments. To simulate the minimum hydrogen supply amounts, we set the constraint condition that the accumulated acetate concentration was less than 0.5 mM and the ultimate nitrate concentration was less than 0.7 mM after treatment. The simulated results were shown in Figure 9. For example, if the initial bicarbonate and nitrate concentrations of the nitrate-contaminated groundwater were 5 and 2.5 mM, the simulated minimum hydrogen supply was 0.2 mmol, and the ultimate nitrate concentration was 0.7 mM after treatment by the co-culture system.

3.5. Implications

In contrast to previous work (Xiao *et al.* 2016), we verified the effect of SO/PS inoculation ratio on acetate accumulation and detailedly examined the effects of substrates concentrations on the denitrification performance in the co-culture system. It is noticeable that the performance of the co-culture system is the result of trade-offs between multiple impacts of individual factors including substrate concentrations and inoculation conditions. For instance, the initial bicarbonate concentration would not only directly affect the growth rate of SO, but also affect the growth rate of PS via acetate concentration. Compared to other multi-species simulations focusing on the effect of process parameters on overall system performance (Chen *et al.* 2016; Kubannek *et al.* 2020), we emphasized the mutual influences between SO and PS. The mutual effects simulations between the two species showed that SO had a significant effect on the denitrification kinetics of PS, while PS had a slight influence on the acetate-producing kinetics of SO. This will help us understand the cooperation relations between the two species and provide useful information for controlling the community populations. The co-culture system performance under different substrate concentration and inoculation ratio was simulated to predict the denitrification performance and further to find the optimal values of these parameters. Additionally, the minimum hydrogen supply was predicted under simulated natural nitrate-contaminated groundwater conditions. These will offer a basis for the further engineering of this co-culture system.

4. CONCLUSIONS

The mathematical model results presented in this study indicated which relationships may be critical for the co-culture system performance and provided the direction for the next round of experiments to test these hypotheses. Simulation results showed that SO had a significant effect on the kinetics of denitrification by PS, while PS slightly affected the kinetics of acetate production by SO. Increasing the SO/PS inoculation ratio would shorten the reaction time for the co-culture system to reach the maximum $\triangle NO_3^-/\triangle H_2$ value; however, the maximum accumulated acetate concentration increased. The co-culture system achieved satisfied performance at initial HCO_3^-/NO_3^- ratio ranging from 0.77 to 1.48. The minimum hydrogen supply was recommended when the bicarbonate and nitrate concentrations were assigned in the range of 2–20 mM and 2–4 mM for simulating the natural nitrate-contaminated groundwater treatment.

ACKNOWLEDGEMENTS

This work was financially supported by the National Natural Science Foundation of China (grant numbers 51908281 and 41807122).

DATA AVAILABILITY STATEMENT

All relevant data are included in the paper or its Supplementary Information.

CONFLICT OF INTEREST

The authors declare there is no conflict.

REFERENCES

Amoako-Nimako, G. K., Yang, X. Y. & Chen, F. M. 2021 Denitrification using permeable reactive barriers with organic substrate or zero-valent iron fillers: controlling mechanisms, challenges, and future perspectives. *Environmental Science and Pollution Research* **28** (17), 21045–21064.

Aoki, K., Toda, H., Yamamoto, J., Chen, J. Y. & Nishiumi, T. 2012 Is hydrogen gas in water present as bubbles or hydrated form? *Journal of Electroanalytical Chemistry* **668**, 83–89.

Capodici, M., Avona, A., Laudicina, V. A. & Viviani, G. 2018 Biological groundwater denitrification systems: lab-scale trials aimed at nitrous oxide production and emission assessment. *Science of the Total Environment* **630**, 462–468.

Chen, X., Guo, J., Xie, G.-J., Yuan, Z. & Ni, B.-J. 2016 Achieving complete nitrogen removal by coupling nitritation-anammox and methane-dependent denitrification: a model-based study. *Biotechnology and Bioengineering* **113** (5), 1035–1045.

Costa, D. D., Gomes, A. A., Fernandes, M., Bortoluzzi, R. L. D., Magalhaes, M. D. B. & Skoronski, E. 2018 Using natural biomass microorganisms for drinking water denitrification. *Journal of Environmental Management* **217**, 520–530.

Di Capua, F., Pirozzi, F., Lens, P. N. L. & Esposito, G. 2019 Electron donors for autotrophic denitrification. *Chemical Engineering Journal* **362**, 922–937.

Epsztein, R., Nir, O., Lahav, O. & Green, M. 2015 Selective nitrate removal from groundwater using a hybrid nanofiltration-reverse osmosis filtration scheme. *Chemical Engineering Journal* **279**, 372–378.

Feng, L., Yang, J., Ma, F., Pi, S., Xing, L. & Li, A. 2020 Characterisation of *Pseudomonas stutzeri* T13 for aerobic denitrification: stoichiometry and reaction kinetics. *Science of the Total Environment* **717**, 135181.

Gao, S., Li, C., Jia, C., Zhang, H., Guan, Q., Wu, X., Wang, J. & Lv, M. 2020 Health risk assessment of groundwater nitrate contamination: a case study of a typical karst hydrogeological unit in East China. *Environmental Science and Pollution Research* **27** (9), 9274–9287.

Garcia-Segura, S., Lanzarini-Lopes, M., Hristovski, K. & Westerhoff, P. 2018 Electrocatalytic reduction of nitrate: fundamentals to full-scale water treatment applications. *Applied Catalysis B-Environmental* **236**, 546–568.

Heijnen, J. J. & Kleerebezem, R., 2010 Encyclopedia of industrial biotechnology: bioprocess, bioseparation, and cell technology. In: *Bioenergetics of Microbial Growth* (Flickinger, M. C. ed.). John Wiley & Sons Inc., New York, NY, USA, pp. 1–23.

Hosseini, S. M., Tosco, T., Ataie-Ashtiani, B. & Simmons, C. T. 2018 Non-pumping reactive wells filled with mixing nano and micro zero-valent iron for nitrate removal from groundwater: vertical, horizontal, and slanted wells. *Journal of Contaminant Hydrology* **210**, 50–64.

Kazemi, M., Biria, D. & Rismani-Yazdi, H. 2015 Modelling bio-electrosynthesis in a reverse microbial fuel cell to produce acetate from CO_2 and H_2O. *Physical Chemistry Chemical Physics* **17** (19), 12561–12574.

Kubannek, F. & Krewer, U. 2019 Modeling and parameter identification for a biofilm in a microbial fuel cell. *Chemie Ingenieur Technik* **91** (6), 856–864.

Kubannek, F., Thiel, S., Bunk, B., Huber, K., Overmann, J., Krewer, U., Biedendieck, R. & Jahn, D. 2020 Performance modelling of the bioelectrochemical glycerol oxidation by a co-culture of *Geobacter Sulfurreducens* and *Raoultella Electrica*. *Chemelectrochem* **7** (8), 1877–1888.

Lazaratou, C. V., Vayenas, D. V. & Papoulis, D. 2020 The role of clays, clay minerals and clay-based materials for nitrate removal from water systems: a review. *Applied Clay Science* **185**, 105377.

Lim, J. X., Zhou, Y. & Vadivelu, V. M. 2020 Enhanced volatile fatty acid production and microbial population analysis in anaerobic treatment of high strength wastewater. *Journal of Water Process Engineering* **33**, 101058.

London, M. R., De Long, S. K., Strahota, M. D., Katz, L. E. & Speitel, G. E. 2011 Autohydrogenotrophic perchlorate reduction kinetics of a microbial consortium in the presence and absence of nitrate. *Water Research* **45** (19), 6593–6601.

Mencio, A., Mas-Pla, J., Otero, N., Regas, O., Boy-Roura, M., Puig, R., Bach, J., Domenech, C., Zamorano, M., Brusi, D. & Folch, A. 2016 Nitrate pollution of groundwater; all right…, but nothing else? *Science of the Total Environment* **539**, 241–251.

Mousavi, S., Ibrahim, S. & Aroua, M. K. 2014 Effects of operational parameters on the treatment of nitrate-rich wastewater by autohydrogenotrophic denitrifying bacteria. *Water and Environment Journal* **28** (4), 556–565.

Picioreanu, C., Head, I. M., Katuri, K. P., van Loosdrecht, M. C. M. & Scott, K. 2007 A computational model for biofilm-based microbial fuel cells. *Water Research* **41** (13), 2921–2940.

Rezvani, F., Sarrafzadeh, M. H., Ebrahimi, S. & Oh, H. M. 2019 Nitrate removal from drinking water with a focus on biological methods: a review. *Environmental Science and Pollution Research* **26** (2), 1124–1141.

Sander, R. 2015 Compilation of Henry's law constants (version 4.0) for water as solvent. *Atmospheric Chemistry and Physics* **15** (8), 4399–4981.

Talalaj, I. A. 2015 Removal of nitrogen compounds from landfill leachate using reverse osmosis with leachate stabilization in a buffer tank. *Environmental Technology* **36** (9), 1091–1097.

Tarhan, C. & Cil, M. A. 2021 A study on hydrogen, the clean energy of the future: hydrogen storage methods. *Journal of Energy Storage* **40**, 102676.

Tsai, H. H., Ravindran, V., Williams, M. D. & Pirbazari, M. 2004 Forecasting the performance of membrane bioreactor process for groundwater denitrification. *Journal of Environmental Engineering and Science* **3** (6), 507–521.

Wang, J. L. & Chu, L. B. 2016 Biological nitrate removal from water and wastewater by solid-phase denitrification process. *Biotechnology Advances* **34** (6), 1103–1112.

Wick, K., Heumesser, C. & Schmid, E. 2012 Groundwater nitrate contamination: factors and indicators. *Journal of Environmental Management* **111**, 178–186.

Wu, J. H. & Sun, Z. C. 2016 Evaluation of shallow groundwater contamination and associated human health risk in an alluvial plain impacted by agricultural and industrial activities, Mid-west China. *Exposure and Health* **8** (3), 311–329.

Xiao, Z., Awata, T., Zhang, D. & Katayama, A. 2016 Denitrification by *Pseudomonas stutzeri* coupled with CO_2 reduction by *Sporomusa ovata* with hydrogen as an electron donor assisted by solid-phase humin. *Journal of Bioscience and Bioengineering* **122** (3), 307–313.

Yang, Y. Y. & Toor, G. S. 2017 Sources and mechanisms of nitrate and orthophosphate transport in urban stormwater runoff from residential catchments. *Water Research* **112**, 176–184.

First received 31 January 2023; accepted in revised form 30 March 2023. Available online 11 April 2023